BOLLETTINO DI GEOFISICA TEORICA ED APPLICATA VOL. 40, N. 3-4, pp. 179-188; SEP.-DEC. 1999

Study of the gravity field spectrum in Canada in view of cm-geoid determination

C. KOTSAKIS and M. G. SIDERIS

Department of Geomatics Engineering, University of Calgary, Alberta, Canada

(Received October 4, 1998; accepted August 5, 1999)

Abstract. The local behaviour of the gravity field spectrum in Canada is studied in this paper, using the EGM96 geopotential model (GM) coefficients, point gravity anomaly data, and Digital Elevation Model (DEM) grids down to spatial resolution of 1 arcmin. The classic FFT-based periodogram method is used to estimate the local covariance and power spectral density functions for various gravity field signals, using gridded gravity and height data. Kaula-type parametric models are fitted to various bands of the local gravity field spectrum in order to model its decay rate. The corresponding covariance functions are also studied in detail through their estimated characteristic parameters. The analysis is done separately for flat and mountainous areas, and the required data grid spacings are derived for dm- and cm-geoid, as well as the estimates for the geoid aliasing error at various data resolution levels. The same analysis is also carried out for relative geoid accuracy at the 1 ppm level or better.

1. Introduction

A high-precision, high-resolution geoid requires a detailed evaluation of the spectral characteristics for all data signals involved in the computational procedure. Such spectral information for various gravity field signals is very useful, since it provides the means to determine realistic signal covariance (CV) models to be used by optimal estimation methods (such as collocation), as well as by data noise propagation studies (Sideris, 1995). Furthermore, empirical determination of the low-wavelength behaviour of the gravity field can offer valuable information for estimating *data resolution requirements* (i.e. the need for a particular local gravity/height grid spacing in order to obtain a certain geoid accuracy level), and may also be utilised for applying general constraints on the spatio-statistical distribution of the earth's crust density anomalies that generate the actual gravity

Corresponding author: C. Kotsakis; Dept. of Geomatics Engineering, University of Calgary, 2500 University Drive N.W., Calgary, Alberta, Canada T2N 1N4; phone: +1 403 2204113; Fax: +1 403 2841980; e-mail: ckotsaki@ucalgary.ca

field; see Forsberg (1984).

In this paper, the behaviour of the local CV function and the associated power spectrum is studied for a variety of gravity field signals in Canada, including (i) local free-air gravity anomalies (Δg), (ii) terrain correction, (iii) their correspondingly implied geoidal undulations, and (iv) geoid indirect effect according to Helmert's second condensation method (Heiskanen and Moritz, 1967; Wichiencharoen, 1982). The high frequency power spectra of all three local geoid components are used to estimate the total geoid aliasing error at various data resolution levels. The study has been performed separately in mountainous and flat test areas in Canada. The local free-air Δg signal and the corresponding free-air geoid have been analysed relative to a high-degree spherical harmonic global field for the anomalous potential of the Earth, which is based on the coefficients of the EGM96 (n_{max}=360) geopotential model (Lemoine et al., 1997) and the GRS80 normal gravity field. This makes comparisons with similar older studies in Canada (see, e.g., Vassiliou and Schwarz, 1985; Schwarz and Lachapelle, 1980) quite difficult in terms of results compatibility, since all of them had used a much lower-degree reference harmonic model (GEM-10, n_{max}=36) for the local gravity data.

2. Data, methodology and computations

2.1. Gravity/height data and test areas

The CV/spectral analysis was performed in eleven 5° × 5° test areas located in various parts of Canada (see Table 1). Two sets of gridded data were originally generated within each test area, namely 1' × 1' free-air (FA) gravity anomalies and 1' × 1' orthometric heights. The selection of the test blocks was based on the sampling density of the Canadian point gravity database that was provided by the Geodetic Survey Division (GSD) of Canada. The areas with the highest and most uniform data density were chosen, in order to minimise gravity interpolation gridding errors. The 1' × 1' height grids were obtained by a simple kriging interpolation algorithm applied to the coarser 5' × 5' Digital Elevation Model (DEM), already available by GSD for all of Canada.

Table 1 - Geographical location of the test areas.

Test Area #	Latitude (°)		Longitude (°)		Location
	Southern	Northern	Western	Eastern	
W1	59	64	-141	-136	North. Cordillera
W2	59	64	-136	-131	North. Cordillera
W3	59	64	-131	-126	North. Cordillera
W4	54	59	-131	-126	North. Cordillera
W6	49	54	-121	-116	South. Cordillera
W13	49	54	-116	-111	South. Alberta
E1	46	51	-79	-74	South. Ontario
E2	46	51	-74	-69	South. Quebec
E5	51	56	-69	-64	North. Quebec
E11	51	56	-89	-84	North. Ontario
E15	46	51	-84	-79	South. Ontario

The selected test areas are divided into two groups, western (W) and eastern (E), which are expected to represent two considerably different realisations of the Canadian gravity field. In the western test areas there is a very strong local gravity signal with high variability due to the large amount of topographic masses that exist there (i.e. Rocky Mountains, Western Northern Cordillera), in contrast to the eastern test areas where the local gravity field is much weaker and smoother. Most of the results presented in section 3 correspond to averages computed for each group (W and E) of the test blocks. In a future paper, test areas that significantly deviate from this averaged spectral behaviour in western and eastern Canada will be identified and studied individually.

2.2. Signal grid computations

The local free-air Δg test grids were referenced to an EGM96-based harmonic model for the anomalous potential, in order to reduce any global trends and to better isolate the local features of the Canadian gravity field. The statistics of these *residual* Δg grids reflected the expected differences between western and eastern Canada. Free-air gravity anomaly values (after subtracting the EGM96-based contribution) ranged between –743 and 543 mGal in the western test blocks, whereas in the eastern areas the range was as low as (-83) - (+118) mGal. The rms signal power ranged from 24 to 72 mGal in the western and from 11 to 14 mGal in the eastern test areas, with the corresponding σ values following a similar pattern. The height statistics for the various test areas are also very representative for the terrain differences between eastern and western Canada. The height rms values varied between 1170 and 1769 m in the six western test blocks, and between 163 and 545 m in the five eastern areas. Maximum height values in the west were as high as 5456 m, whereas the highest altitude in the east was 1507 m.

Terrain correction (TC) values were computed in each test grid using the 2D planar Fast Fourier Transform (FFT) algorithm. The computations were carried up to the 3rd order term of the Taylor series expansion, and the mass-prism topographic model was used; for details and mathematical formulas, see Li and Sideris (1994). In the western test blocks the terrain correction signal showed an average behaviour of about 12 mGal (rms), with maximum values up to 155 mGal! On the other hand, the terrain correction rms power in the eastern test areas was only 0.5 mGal on the average, with the largest values not exceeding the 20 mGal limit. Finally, the geoid indirect effect was computed by the 2D planar FFT formulae. The zero, first, and second order terms of the Taylor series expansion have been computed according to the formulation of Wichiencharoen (1982). The statistics of the geoid indirect effect grids also showed a remarkable difference between western and eastern Canada. The average rms power in the west was approximately 14.5 cm, whereas in the east it was only 0.8 cm. The largest geoid indirect effect values were -170 cm and -13 cm for the western and eastern test blocks, respectively.

2.3. Methodology for CV/spectral analysis

The 2D planar CV and power spectral density (PSD) functions of the various signals (residual

free-air Δg, terrain correction, and geoid indirect effect) were estimated using the classical FFT-based periodogram approach. Some windowing was also applied to all signal grids in order to reduce leakage effects; for details and formulas regarding the CV/PSD estimation procedure, see Vassiliou and Schwarz (1985). In accordance with an *isotropic assumption* for the behaviour of the local gravity field, the resulting 2D CV and PSD functions were then radially averaged into their 1D isotropic counterparts. Some indication for the anisotropy level of the various local gravity field signals will be given in the following section through an *anisotropy index* η, which is simply defined as the ratio between the maximum and minimum correlation lengths of the 2D CV functions (Forsberg, 1986). The 1D isotropic PSDs were finally converted into a discrete 'local spherical spectrum', using the asymptotic relationship derived by Forsberg (1984):

$$c_n = (2\pi R^2)^{-1}(n+0.5)PSD(\omega), \;\; \omega = R^{-1}(n+0.5) \tag{1}$$

where $PSD(\omega)$ is the 1D isotropic planar PSD (of the signal under consideration) evaluated at the radial wavenumber ω, c_n are the corresponding 'local degree variances' at the harmonic degree n, and R is the mean radius of the Earth. The extent and the grid spacing of the test areas define the minimum (n_{min}) and the maximum (n_{max}) recoverable harmonic degree of the power spectrum, which in our case are 72 and 10 800, respectively. From the c_n of the residual free-air Δg and the terrain correction signals, the corresponding geoid degree variances (k_n) were also computed using the classic spectral formula (Heiskanen and Moritz, 1967):

$$k_n = R^2 \frac{c_n}{\gamma^2 (n-1)^2} \tag{2}$$

where γ denotes a mean gravity value on the surface of the Earth. A simple Kaula-type parametric formula (i.e. $k_n = A/n^x$) was also used, through a least-squares fitting, to model the decay of all the signal power spectra and to estimate the lost gravity/geoid power from the unrecoverable spectral band $n > 10\,800$.

Finally, a parameter of special interest for geoid computations is the *short-wavelength geoid power* m_N, i.e. the rms value of the local geoid signal contributed above a certain large harmonic degree n_o,

$$m_N^2(n \geq n_o) = \sum_{n=n_o}^{\infty} k_n = R^2 \gamma^{-2} \sum_{n=n_o}^{\infty} (n-1)^{-2} c_n \;\; . \tag{3}$$

The computation of m_N at various n_o reference values, corresponding to selected grid resolution levels (e.g. 10', 5', etc.), can provide a valuable picture of the aliasing effects on the local geoid and a useful means to assess data resolution requirements in view of cm-level geoid accuracy. Three different m_N values were computed for every selected n_o, which correspond to the three different geoid components (free-air geoid, TC geoid, indirect effect) originating from the use of the local gravity and height data. For harmonic degree values n above n_{max}=10 800, the previous formula (3) was evaluated with the help of a best fitted Kaula-type parametric model. Various estimates of the *total* geoid aliasing error will be given in the next section, in both an absolute and relative sense.

Table 2 - Local covariance function parameters for various gravity field signals.

	Residual Free-Air Δg			Terrain Correction			Geoid Indirect Effect		
	σ^2 (mGal^2)	ξ (arcmin)	η	σ^2 (mGal^2)	ξ (arcmin)	η	σ^2 (cm^2)	ξ (arcmin)	η
Western Canada									
Min	569.77	4.24	1.4	14.37	4.85	1.2	24.98	5.32	1.2
Max	5174.80	10.48	3.3	153.81	14.89	2.9	158.98	17.03	3.5
Average	2659.59	6.38	1.8	56.18	8.42	1.6	82.28	9.95	1.8
Eastern Canada									
Min	43.31	6.50	1.2	0.00	3.29	1.3	0.02	7.35	1.0
Max	207.01	8.04	1.5	0.54	20.99	1.8	0.56	45.69	3.2
Average	112.30	7.21	1.3	0.17	10.18	1.6	0.23	25.17	1.7

3. Analysis of results

3.1. Local CV functions

The estimated values for the three basic parameters that describe the behaviour of the local CV function for (i) residual free-air Δg (ii) terrain correction, and (iii) geoid indirect effect, are given in Table 2. The differences between the mountainous western areas and the flat eastern areas are seen in the variance (σ^2) and correlation length (ξ) values. A very strong topographic attraction signal around the Rocky Mountains test areas causes the variance of the residual free-air Δg to be ~2660 mGal^2 on the average, compared to an average low of ~112 mGal^2 in the eastern test blocks. These regional differences are much more pronounced in the terrain correction and indirect effect signals. In a similar study (Schwarz and Lachapelle, 1980), an estimate for the FA anomaly variance was given for non-mountainous Canadian areas in the order of 467.4 mGal^2, which clearly disagrees with the σ^2 estimates obtained for the flat areas of our study. Such a difference should be attributed to the use of a lower quality/resolution reference harmonic global model (GEM-10, n_{max}=36) by the older study, as well as to the incorporation of much more sparse local gravity data than currently exist in the GSD database.

Signal variability differs also significantly between the two test groups. The ξ values for all signals are consistently smaller in the western areas, reflecting the higher frequency content of the gravity field there. In Schwarz and Lachapelle (1980) the estimated value for the correlation length in the free-air Δg signal for flat areas was 25', which deviates from our corresponding estimate (7.2') due to the smoothing effect caused by the use of mean 5' × 5' gravity data in the older study. Finally, the computation of the anisotropy index η showed that there are cases where an isotropic assumption cannot be validated. However, even after the radial smoothing of the 2D CV and PSD functions, we

Table 3 - RMS power and spectral decay for the local geoid signal components.

	***N* from Residual Free-Air Δg**			***N* from Terrain Correction**			***N* from Indirect Effect**		
	RMS (cm)	**k_n decay slope (x)**		**RMS (cm)**	**k_n decay slope (x)**		**RMS (cm)**	**k_n decay slope (x)**	
		$n > 72$	$n > 360$		$n > 72$	$n > 360$		$n > 72$	$n > 360$
Western Canada									
Min	33.9	3.9	4.3	8.4	3.7	4.1	5.0	2.1	2.2
Max	213.6	4.5	5.0	40.9	4.2	4.5	12.6	2.5	2.8
Average	119.6	4.2	4.5	25.1	4.2	4.5	9.1	2.2	2.5
Eastern Canada									
Min	9.9	3.9	4.5	0.0	2.8	2.4	0.1	1.8	1.6
Max	21.9	4.4	5.0	3.1	3.8	3.9	0.7	2.4	2.6
Average	16.3	4.3	4.8	1.8	3.7	3.9	0.5	2.4	2.6

are still able to extract important information for the average spatial behaviour of the various gravity field signals.

3.2. Local geoid RMS power and spectral decay rate

In Table 3, the rms power (in cm) is given for the various local geoid components. These values have been computed through the estimated geoid degree variances k_n (for each test area and data set) in the recoverable spectral band $72 \le n \le 10\,800$, as well as through the *modelled* k_n in the upper band $n > 10\,800$. In Figs. 1 and 2, the estimated degree variances for the various local geoid components (averaged over all western and eastern test areas respectively) are shown, together with the global geoid power spectrum according to the EGM96 geopotential model. The actual 'source' data (i.e. residual free-air Δg, terrain correction) in the western test areas showed a quite significant amount of rms power in the upper spectral band ($n > 10\,800$), namely 6.2 mGal for Δg and 1.3 mGal for the TC. However, the geoid equivalencies of these two high-frequency contributions are almost negligible (< 1 cm). The importance of proper terrain modelling for geoid computations in mountainous areas is also evident from Table 3. Terrain correction alone can create a geoid signal of ~25 cm on average, while the indirect effect contributes an additional component of 9-10 cm (rms). The corresponding values for the flat eastern areas show that such topographic effects should always be taken into account, if a 'true' cm-geoid is desired.

The decay rate of the local geoid power spectrum (expressed by the value of the exponent x in the parametric model $k_n = A/n^x$) is also given in Table 3, for only two of the various spectral bands used in the least-squares fittings. The geoid degree variances k_n originating from the residual free-air Δg and the terrain correction (see Figs 1 and 2) seem to follow a faster decaying pattern than the

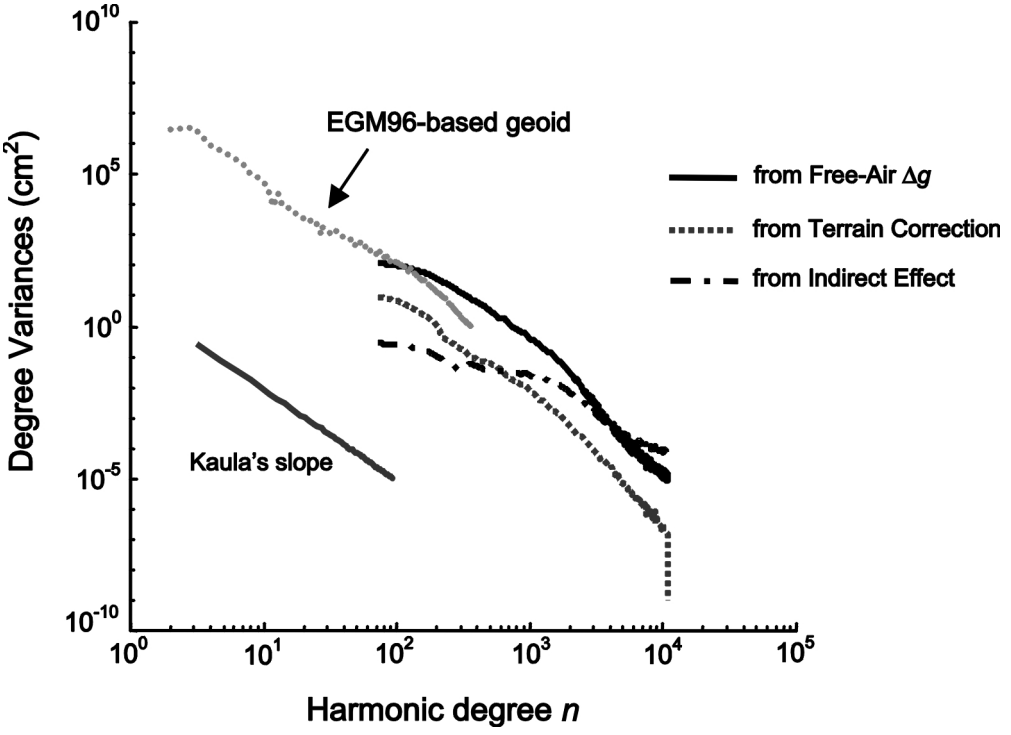

Fig. 1 - Power spectrum for various local geoid components (Western Canada).

Kaula rule implies ($x \approx 3$), which agrees with similar indications given in older studies in Canada (Vassiliou and Schwarz, 1985) and in northern Europe (Forsberg, 1986). Actually, this decaying pattern for the two local geoid components is also in good agreement with the decay rate of the EGM96-based global geoid degree variances, in the case where the global harmonic model is restricted to its upper band $180 < n < 360$ ($x = 4.6$). On the other hand, the k_n of the third geoid component (indirect effect) seems to decay at a slower rate than Kaula's rule (see Table 3), but more analysis with denser height data is needed to validate such a conclusion since possible aliasing effects in the spectrum estimation may be responsible for this behaviour.

It is finally interesting to mention the significant amount of low-wavelength power that the geoid indirect effect showed for harmonic degrees $n > 700$ in the western test areas. It completely dominates over the local geoid signal originating from the TC, and it is even stronger than the local free-air geoid for $n > 4000$ (see Fig. 1). In particular, the indirect effect showed an rms value of ~5.4 cm inside the spectral band $720 < n < 10\,800$, while the geoid component stemming from the terrain correction in the same band has an rms power of ~2.5 cm. The local free-air geoid is at the 3 cm level over the spectral band $2160 < n < 10\,800$, but it is much stronger in the lower band $1080 < n < 2161$, where it gives an 11 cm geoid signal component. All the corresponding values for the eastern test areas are almost negligible.

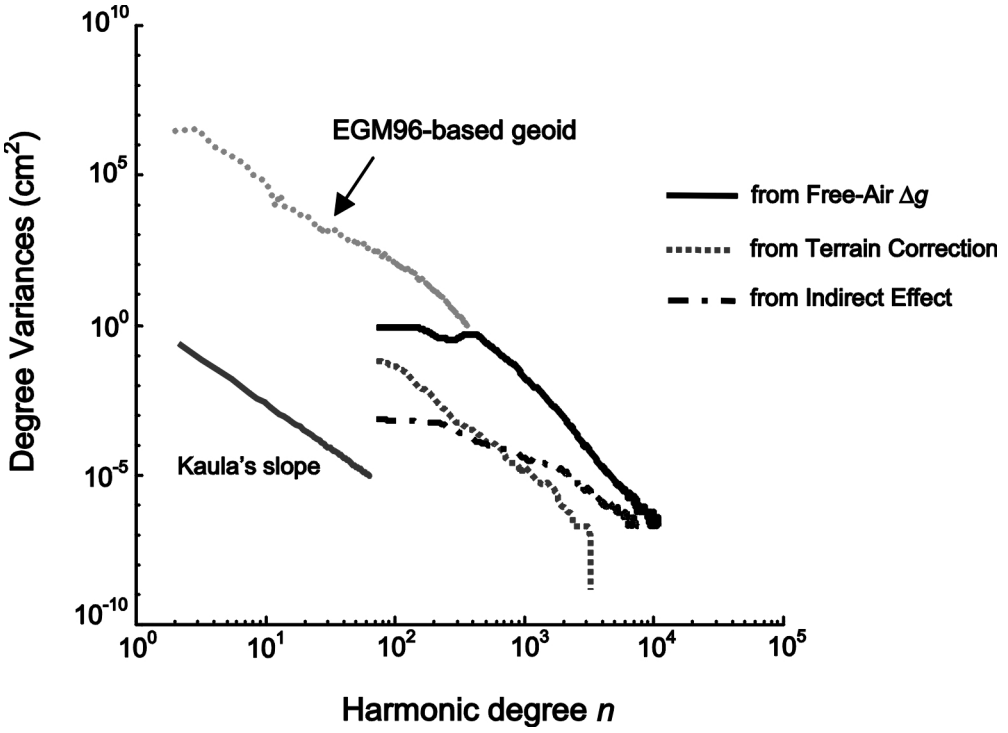

Fig. 2 - Power spectrum for various local geoid components (Eastern Canada).

3.3. Geoid aliasing error

Using the local geoid degree variances k_n from the three different sources (residual free-air anomalies, terrain correction, indirect effect), various estimates for the total geoid aliasing error have been computed at standard data resolution levels. These results are given in Table 4. Note that all values correspond to averages computed over the different test areas in western and eastern Canada. Two extreme cases were considered in order to easily compute the total error from the individual aliasing errors in the three geoid components, namely (i) all three individual local geoid components are uncorrelated, and (ii) a perfect (linear) correlation exists for all combinations among the three local geoid components. Since all local geoid components depend (directly or indirectly) on the topography, some considerable correlation among them should be expected, and more weight should be put in the values of the second case. The required gravity/height data resolution in western Canada for cm-geoid was estimated to be ~1.5', and for dm-geoid ~7'. In the eastern parts of Canada, dm-geoid accuracy is achieved without even taking terrain effects into account, by using a local gravity grid spacing of ~25'. For cm-level geoid, gravity and terrain data should be combined with a resolution better than 7'. Note that all the above estimates refer to perfect (noiseless) data and they correspond to an average spatial behaviour (rms accuracy). Individual 'pointwise' geoid errors may vary (even considerably in some cases) from these values.

In view of the increasing need for high *relative* geoid accuracy for GPS/levelling applications

Table 4 - Geoid RMS aliasing errors at various local data resolution levels (all values in cm).

Local Data Resolution Level	Zero correlation among $N_{\Delta g}$, N_{TC}, N_{IND}				Perfect correlation among $N_{\Delta g}$, N_{TC}, N_{IND}			
	Geoid resulting from EGM96 & Free-air Δg only		Geoid resulting from EGM96 & Free-air Δg & terrain effects		Geoid resulting from EGM96 & Free-air Δg only		Geoid resulting from EGM96 & Free-air Δg & terrain effects	
	West	East	West	East	West	East	West	East
30' × 30'	47.35	10.58	40.00	10.42	73.31	12.72	50.82	10.98
15' × 15'	32.53	4.51	19.54	4.12	52.79	6.41	26.57	4.43
10' × 10'	28.98	2.76	12.19	2.04	45.47	4.33	17.16	2.20
5' × 5'	26.86	1.93	3.83	0.50	37.18	2.79	5.71	0.59
1' × 1'	26.70	1.87	0.68	0.00	34.37	2.30	0.83	0.00

(see, e.g., Forsberg and Madsen, 1990), the 'absolute' aliasing error values of Table 4 were finally transformed into relative geoid error variances and the resulting values are given in Table 5. Only the worst case of perfect correlation among the various local geoid components has been considered. Three typical baseline lengths (10/50/100 km) have been used for the ppm normalisation. It is seen that a relative geoid accuracy of 1 ppm in western Canada, for small baseline lengths, can only be achieved through the use of very high resolution (< 1') gravity grids and DEMs. For larger baselines, ppm and even sub-ppm accuracy seems possible, if the gravity/height data resolution is not worse than ~5'. In eastern Canada, we can obtain a 1-ppm relative geoid for small baselines only if we take into account all the terrain effects with a data grid resolution better than 6'-7'. The weak short-wavelength structure of the gravity field in the same areas, however, makes the sub-ppm relative geoid over larger baselines possible with the use of lower resolution (> 10') data grids.

4. Summary and conclusions

In the present paper, the spectral characteristics of the gravity field in Canada have been studied

Table 5 - Relative geoid error as a function of local gravity/height data density (all values in ppm).

Data resolution	10 km baseline				50 km baseline				100 km baseline			
	N without terrain effects (West / East)		*N* with terrain effects (West / East)		*N* without terrain effects (West / East)		*N* with terrain effects (West / East)		*N* without terrain effects (West / East)		*N* with terrain effects (West / East)	
30' × 30'	103.7	18.0	71.9	15.5	20.7	3.6	14.4	3.1	10.4	1.8	7.2	1.6
15' × 15'	74.7	9.1	37.6	6.3	14.9	1.8	7.5	1.3	7.5	0.9	3.8	0.6
10' × 10'	64.3	6.1	24.3	3.1	12.9	1.2	4.9	0.6	6.4	0.6	2.4	0.3
5' × 5'	52.6	3.9	8.1	0.8	10.5	0.8	1.6	0.2	5.3	0.4	0.8	0.1
1' × 1'	48.6	3.2	1.2	0.0	9.7	0.6	0.2	0.0	4.9	0.3	0.1	0.0

in terms of a number of key parameters (variance, correlation length, anisotropy index, local geoid degree variances, short-wavelength rms power for the various local geoid components) using gravity and height gridded data. Absolute and relative geoid accuracy estimates (as a function of local data density) have been computed, as well as grid resolution requirements for a cm/dm/ppm/sub-ppm geoid. It should be emphasised that these accuracy values do not represent the overall geoid quality, since the errors associated with the gravity/height data and the geopotential model (EGM96) coefficients have not been taken into account. Similar methodology, to the one presented here, can be applied in order to study and model the error CV and PSD functions for the various data sets, but more theoretical developments are needed to overcome the important non-stationary noise problem in spectral gravity field modelling (Sideris, 1995). The use of larger and denser (< 1') data grids can also improve the gravity field spectrum estimates, at both high and low wavelength bands. Finally, the incorporation of density data in the spectral analysis procedure will help to identify the significance of the classic constant-density assumption towards the cm-geoid challenge.

Acknowledgements. This research was funded by a contract from the Geodetic Survey of Canada and by an International Research Fellowship awarded to the second author by Germany's Alexander von Humboldt Foundation. The paper was also presented at the *2nd Joint Meeting of the International Gravity Commission and the International Geoid Commission*, held in Trieste, Italy, September 7-12, 1998.

References

Forsberg R.; 1984: *Local Covariance Functions and Density Distributions.* Report No.356, Dept. of Geodetic Science and Surveying, Ohio State University, Columbus, Ohio.

Forsberg R.; 1986: *Spectral Properties of the Gravity Field in the Nordic Countries.* Boll. di Geod. e Sci. Affi., **4**, 361-383.

Forsberg R. and Madsen F.; 1990: *High-Precision Geoid Heights for GPS Levelling*. In: Proceedings of the 2nd International Symposium on Precise Positioning with the Global Positioning System, Sept. 3-7, Ottawa, Canada, 1990, pp. 1060-1074.

Heiskanen W. A. and Moritz H.; 1967: *Physical Geodesy.* W. H. Freeman, San Francisco.

Lemoine F. G., Smith D. E., Smith R., Kunz L., Pavlis E. C., Pavlis N. K., Klosko S. M., Chinn D. S., Torrence M. H., Williamson R. G., Cox C. M., Rachlin K. E., Wang Y. M., Kenyon S. C., Salman R., Trimmer R., Rapp R. H. and Nerem R. S.; 1997: *The development of the NASA, GSFC and NIMA Joint Geopotential Model*. In: Proceedings of the IAG International Symposium on Gravity, Geoid and Marine Geodesy, Sept. 30 - Oct. 5, Tokyo, Japan, 1996, Springer, vol.117, pp. 461-470.

Li Y. C. and Sideris M. G.; 1994: *Improved gravimetric terrain corrections.* Geophys. J. Int., **119**, 740-752.

Schwarz K. P. and Lachapelle G.; 1980: *Local Characteristics of the Gravity Anomaly Covariance Function*. Bull. Geod., **54**, 21-36.

Sideris M. G.; 1995: *On the use of heterogeneous noisy data in spectral gravity field modelling methods.* Journal of Geodesy, **70**, 470-479.

Vassiliou A. and Schwarz K. P.; 1985: *Study of the high frequency spectrum of the anomalous gravity potential.* Paper presented at the 13th Moving Base Gravity Gradiometer Review, U.S. Air Force Academy, Colorado Springs, February 12-13, 1985.

Wichiencharoen C.; 1982: *The Indirect Effect on the Computation of Geoidal Undulations.* Report No.336, Dept. of Geodetic Science and Surveying, Ohio State University, Columbus, Ohio.